COMPUTER GENERATION OF METAL COMPONENTS BY SIMULTANEOUS DEPOSITION OF MOULD, CORES AND PART

Masoud M. Mohebi, ShoufengYang and Julian R.G. Evans
Department of Materials, Queen Mary, University of London,
Mile End Road, London, E1 4NS, UK

Abstract

A new solid freeforming method based on co-delivery of mould powder materials and part powder materials using vibration-controlled, dry powder valves is presented in this paper. Thin layers of stainless steel powder are delivered to the forming area according to the cross-section of the CAD file to produce the component. Mould powder which has low sinterability is delivered to the non-forming areas of the same layer. All powders are delivered by computer-controlled, acoustic powder valves. The flow rate and switching of the valves provides the composition and shape control during fabrication. The stacked layers of loose powder are then sintered in a conventional furnace. The mould materials are removed after sintering. This method avoids the high thermal stress problem in selective laser sintering, avoids high capitalisation, makes use of conventional furnaces and allows for the incorporation of three dimensional function gradients. Test pieces including step wedge and Spierpinski's cube were fabricated. Advantages, limitations and problems are discussed.

Introduction

Solid freeforming (SFF), reviewed by Pham and Gault [1] among others, is defined as the construction of a three dimensional shape by point, line or planar addition of material without confining surfaces other than a base [2]. In existing SLS, the same material is used in the forming areas and non-forming areas. The material in the non-forming areas is used to support the next layer. Powder in the forming areas is fused by laser scanning. Normally the materials in the non-forming areas are difficult to recycle due to the thermal history. The selective laser sintering process involves wide temperature ranges, rapid cooling and oxidation problems. Furthermore the generation of residual stresses is an inevitable consequence of one layer solidifying upon its predecessor [3, 4]. We therefore devised a method of assembling a complex shape capable of having 3D compositional gradients and for which conventional sintering could be applied. As with SLS, there would still be restrictions on compositional range and on compatibility of powders. These are set by the demands of co-sintering, but the procedure would be much simpler. It would allow for compaction if required. Furthermore, advanced fast sintering methods such as spark plasma sintering (SPS) [5] or induction sintering [6] would be able to co-sinter a wide range of compositions and may improve compatibility.

The emergence of the second generation of solid freeform fabrication methods requires techniques of dispensing multiple materials on a powder bed before laser sintering in SLS or binder printing in 3DP. Various powder mixing and dispensing methods have been studied in the

past few years, such as discrete multi-powder positioning [7], removal of unsintered powder by vacuum suction [8], powder dispensing robot [9], powder ejected by piston and weighting by resonance measurement [10], vibration method [11,12, 13, 14, 15, 16], and electrostatic method [17, 18, 19]. Rock and Gilman [20, 21] describe a system in which two types of powder, one acting as the part powder and one as a support powder that also defines the shape of the part are deposited in each layer. The method of achieving this is not recorded and the description refers throughout to a 'deposition effector' which is not defined. Pegna et al. [22, 23], inspired by the ancient sand-painting art, presents a method of making complex shapes from construction materials that cannot be realised by casting. A similar approach has been used to produce conventionally sintered components, which can include 3D functional gradients, by using acoustic powder feeding of the part and mould powders concurrently [24]. In each layer, the forming area is made of the part powder or mixtures of powder of computer-defined composition and the non-forming areas consist of a mould powder which can later be removed. In this way, it is not necessary to sinter or melt each layer as in SLS, but rather, the whole assembly can be sintered in a conventional furnace such that the mould powder retains the shape of the part. Thus strategies for fully three dimensional functionally graded components based on powder technology are beginning to emerge. In this paper, the fabrication of test pieces including step wedge and Spierpinski's cube (Menger's sponge) were demonstrated.

Experimental Details

The powders were gas atomized grade 420 stainless steel (16-63μm, ex Osprey Metals, Neath, Wales), alumina (BACO Chemicals, Batch: C731 UNG Al_2O_3, BA Chemicals Ltd, Buckinghamshire, UK.), copper (63-212μm, ex Osprey Metals, Neath, Wales) and graphite (GS150-E, GrafTech, UCAR Carbon Co., USA). The properties of powders were listed in Table 1.

Table 1. Properties of powders*

Powder	True density /kg.m^{-3}	Tap density /kg.m^{-3}	Loose density /kg.m^{-3}	Angle of repose/ °	Hall flow meter test /s (50g)
Stainless steel	8000	4600±200	4120±200	29±3	29.5±2.5
Graphite	2100-2200	530±100	500±100	49±3	No flow
Alumina	3970	1480±300	1350±300	33±2	88.3±4.8

*Errors are 95%CL

The powder delivery device consisted of glass capillary tubes of inside diameter 300–660 μm. This diameter range of capillary tubes gave on/off switching and flow rate control for the test powders used. Acoustic vibration was provided by 25mm miniature bass drivers. The cone centres of these were connected to the ends of the tubes by 1mm diameter and 40-50mm length rods. The vibration was supplied from a 2×30 watt amplifier by sound generated using software and

converted into analogue signal by a DA card on a personal computer. The detail of the powder dispensing device is shown elsewhere [25]. A 3D table was driven through 6K4 controller and motion planner software interfaced through labview. The flow rate of powder was measured using a four place balance interfaced to the PC. The reading of the balance was recorded every second. Rectangular graphite crucibles (89mm×33mm×33.5 mm, inside dimension) were machined from stock (GrafTech, UCAR ltd, Sheffield, UK) and provided with a close-fitting base capable of sliding in the 'Z' direction to provide the building platform. The schematic diagram of the equipment and the powder delivery device are shown in figures 1 and 2, respectively.

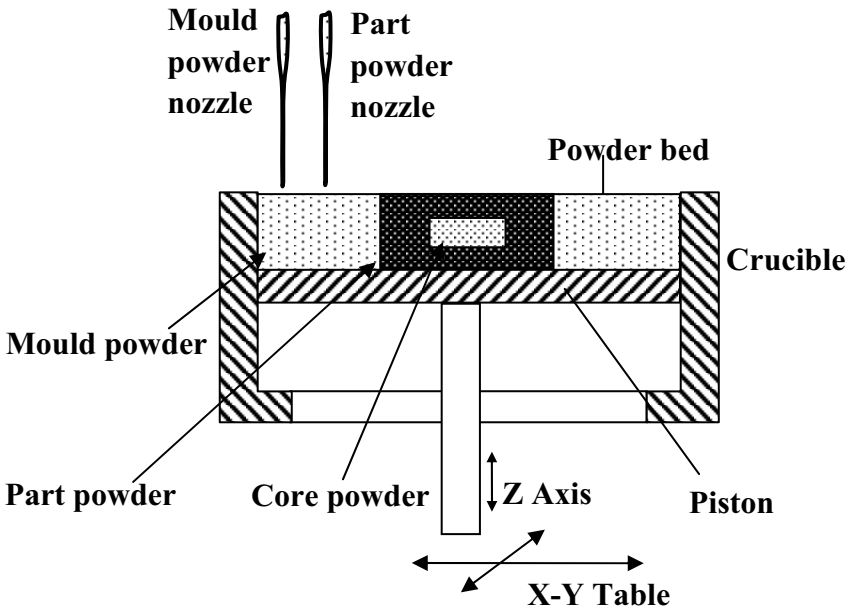

Figure 1. Schematic diagram of powder delivery into a crucible fitted with building platform.

All the experiments were performed at 20-25°C and under 30-60% RH, a region known to provide little variation in flow properties (Matei et al. 1973). The samples were partly sintered in flowing Ar+4%H2 at 1000-1100°C and infiltrated with bronze at 1100°C. Sintered parts of stainless steel were cut, polished and inspected for carborization based on ASTM E407-99 for etching for detection of carbides. Electrolytic etching using a solution of ~10wt% ammonium persulphate in water at 6 V for 30 s was carried out (specimen as anode).

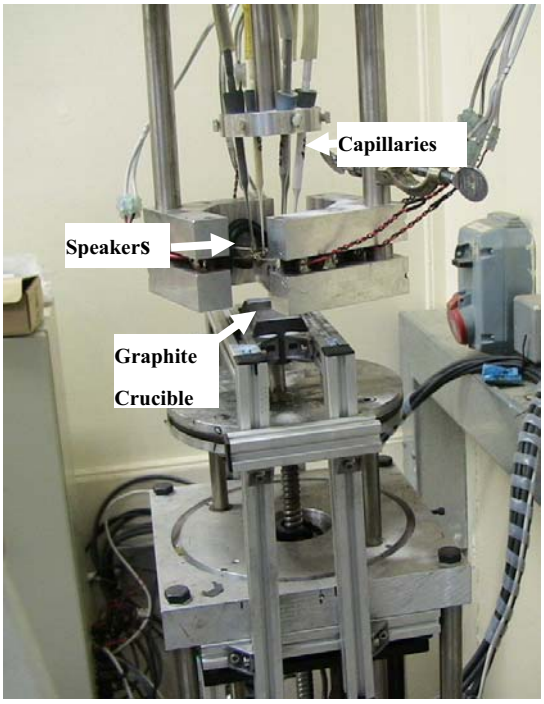

Figure 2 The equipment for dual powder delivery. Six capillaries were installed of which 2 were used in this experiment.

Results and discussion

1. Compatibility of mould and part powders.

In selective laser sintering, an entire layer is placed on the platform and the part powder is selectively laser fused while powder in the non-forming areas remains in the loose state. However in the present method, both the part powder and the mould powder remain in the loose state before entering a conventional sintering furnace. The part powder is either sintered or partly sintered at a temperature where the mould powder remains loose. The compatibility of the mould powders and part powders needs to be considered. The requirements are **a)** the mould powder must have a higher sintering temperature than the part powder; **b)** the two powders should have low reactivity; **c)** the mould powder should be capable of easy and total removal after sintering; **d)** the powder should be sufficiently free-flowing to allow its flow to be arrested and regulated by the acoustic valve. An additional requirement of core powder compare with the mould powder is that it should be able to "collapse" to avoid hot cracks analogous to the requirement of the cores in sand casting. From the experimental results, the mould materials fulfilled the extra requirement as core materials so we adopted same materials as mould and core materials in this paper. The operation of the valve and powder characteristics that allow successful metering and dispensing have been discussed elsewhere [14,26].

Both coarse alumina powder and graphite powder were tested as the mould/core material. Loose copper powder and alumina powder were loaded into an alumina crucible with a thin paper partition which was carefully removed before sintering. These powders were also loaded into a compression die with a thin paper partition which was carefully removed and the assembly pressed at 80 MPa. The interface of non-pressed copper is fairly smooth while in the pressed one, the compaction behaviour, which can be assessed by instrumented die pressing of each powder [27] , is not a perfect match and as a result, the interface between the two powders is slightly distorted after pressing. The non-pressed and pressed copper/alumina samples were then sintered in a furnace at 1050°C for 3 hours with a reducing atmosphere (Ar - 4%H_2). The alumina powder was not sintered at all. The copper could be easily cleaned although there were some alumina particles embedded in the surface. The sintered samples were examined using SEM and backscattered electron mapping of aluminium (**Figure 3**). The pressed sample was sintered to quite high density while the non-pressed was just weakly bonded. In the pressed copper there was a thin layer of entrapped alumina power. The problem presented by the alumina powder entrapped at the surface is that it is difficult to remove the last few grains from sintered parts. Some of the alumina particles appear to be mechanically locked at the surface. Since alumina has a hardness of 2050 kg/mm^2 (Knoop indenter), attempts to finish by conventional tooling are impeded although shot blasting with an abrasive powder may be effective.

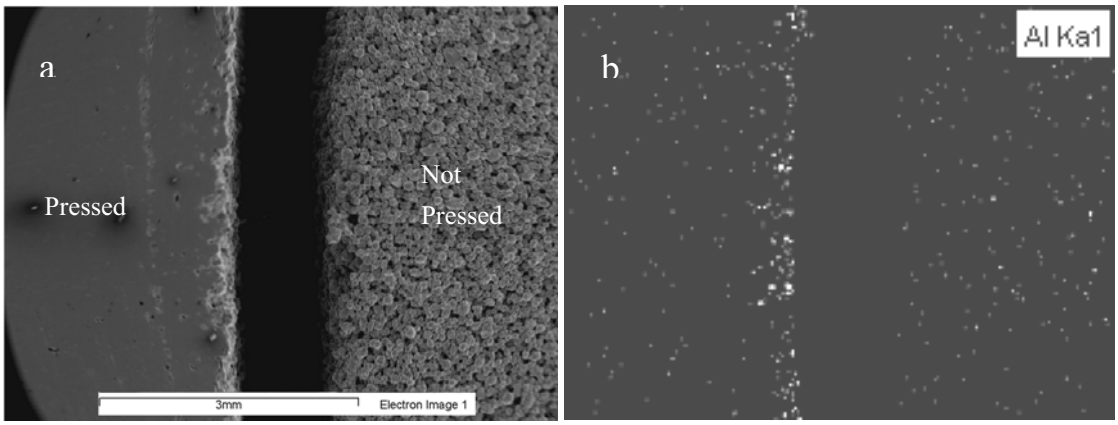

Figure 3: (a) SEM and (b) backscattered electron mapping of aluminium atoms of 2 sintered specimens of pressed (left) and non-pressed (right) cupper powder. Bright line in (b) indicates the entrapment of alumina powders in the pressed copper part. Contamination of alumina in body section of the samples is due to spread of alumina powder throughout the porous specimen in the wet cutting processes for SEM.

Graphite was also tested as a mould material. Loose stainless steel powder and graphite powder were loaded in an alumina crucible with a thin paper partition which was carefully removed before sintering. Then the sample was sintered in a reducing atmosphere (Ar - 4%H_2) at 1100 °C for 1-2 hours. The low loose density and flowability of graphite gives problems when more layers are deposited; the graphite powder has greater compaction ability than steel powder. After multi-layer deposition, the denser steel powder on top of the graphite tends to compress it

more than the neighbouring steel. This may cause distortion of previous layers as the steel powder sinks into previous graphite layers. The main disadvantage of graphite is the possibility of carbon pick-up by ferrous alloys, which is shown in Figure 4. The depth of the carburization is 100-200μm from the interface. No carburization was detected in the central region of the samples.

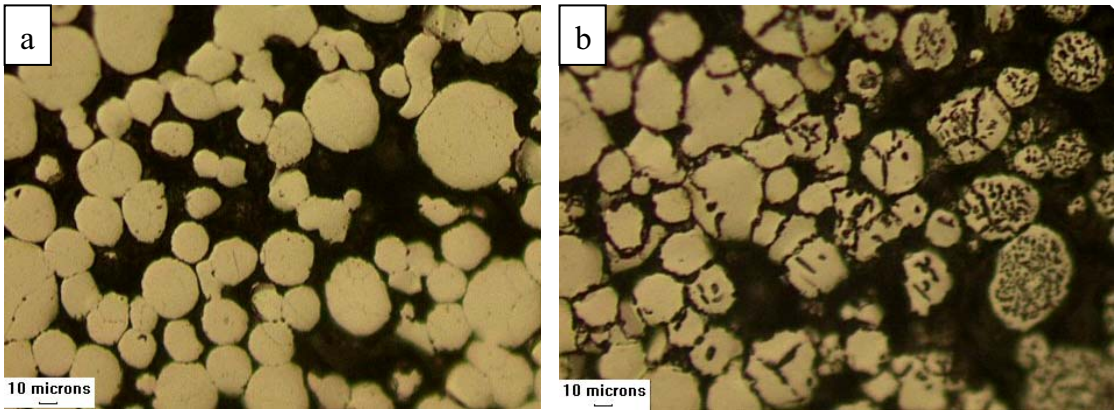

Figure 4: Optical micrograph of partially sintered stainless steel with graphite powder as mould after electrolytic etching to reveal the carbides. The bulk samples do not show carburization (a) but it is detected on the surface adjacent to graphite powder (b).

There are several approaches for removing the mould powder. It can be achieved simply by mechanical detachment, by a gas phase reaction that does not affect the part or by dissolution in a suitable solvent or reactant for which the part material is neither soluble nor reactive.

2. Flow rate and composition control

The flow rate of the powder can be controlled over a wide range by varying the tube diameter, vibration frequency and vibration amplitude. At low frequencies and amplitudes, domes form in the tube and flow stops. The valve can thus provide flow rate control as well as switching. Previous experiments [26] on the effect of tube diameter on flow arrest indicated that if the ratio of tube radius R, to particle radius r, was such that $2<R/r<5$, flow arrest occurred when vibration ceased. A model was established and an equation was derived which provides a reasonable analytical prediction of the experimental flow rate given the complexity of the flow regime [28]. In the open-capillary valve, flow rate approximates to a function of reciprocal amplitude and the gradients show that flow rate doubles for only 20% increase in tube diameter.

Benefitting from a wide range of flow rate control by varying the tube diameter, vibration frequency and vibration amplitude, the powder dispensing device can be constructed either for single materials with several tubes of different diameter or for tubes holding different materials. A dry powder dispensing device with 6 valves was constructed and shown in **Figure 2**. More valves

could be mounted with optimized spacing arrangement. With this multi-valve dry powder deposition device, on-line materials mixing and pattern deposition was achieved [25]. Colour sand paintings with 5 different colour sands have been made to demonstrate the feasibility of multi materials deposition [29].

3. Test piece fabrication

The materials could be either vector scanned or raster deposited [30]. To avoid the errors in the on/off control and improve the dispensing efficiency, the layers were vector scanned to fill the areas (Figure 5). The quality of the build is influenced by the fill strategy. In the early stages of this investigation, the areas were filled with rectangular spirals or zigzags. Examination of the building sites showed that particles were piling up at the turning points as shown in Figure 5 (c) and (d). The diagonal lines seen in these steel powder beds are due to pile-up at the right angle bends. This is caused by the low acceleration and deceleration rate at the turning points, which was needed to avoid shaking the three-axis table and disturbing the powder assembly. While the displacement speed of the table at the turning point is lower than the speed during straight line deposition, the flow rate of the powder is constant. Although it is possible to reduce the flow rate at the tuning point, the response of the flow rate is slow compared with that of the 3D table and the programming of the vibration parameters is complex. This looks acceptable for one or two layers but during multi-layer deposition, this defect can be magnified into seriously uneven surfaces, as can the defect caused by the track distance. To avoid this defect, curved turning points and uniform XY table speed were used wherever possible [24].

To fill a powder blanket properly, the track width and track distance in the same material zone and the track distance between adjacent mould and part materials determine subsequent distortion of the pattern. Improper filling gives an uneven powder bed surface which accumulates into serious inaccuracies after multiple layers of powder deposition. The track width was affected by powder properties, flow rate, nozzle to powder bed distance, and vibration conditions. A study on track width is described elsewhere [25]. The track distance between mould powder and part powder is extremely important in providing for a smooth and well-defined internal part surface. A large track distance between mould and part materials produces a valley as illustrated in Figure 6(a). Conversely, a small track distance produces a hill as illustrated in Figure 6(b). This kind of defect in the powder bed is difficult to observe in the initial stage of deposition but becomes magnified into a serious problem during the fabrication of a vertical wall. An example of the hill effect is shown in Figure 6(d). At the top surface of the sample, the edge adjacent to the mould powder was piled up due to a small track distance between the part and mould powders.

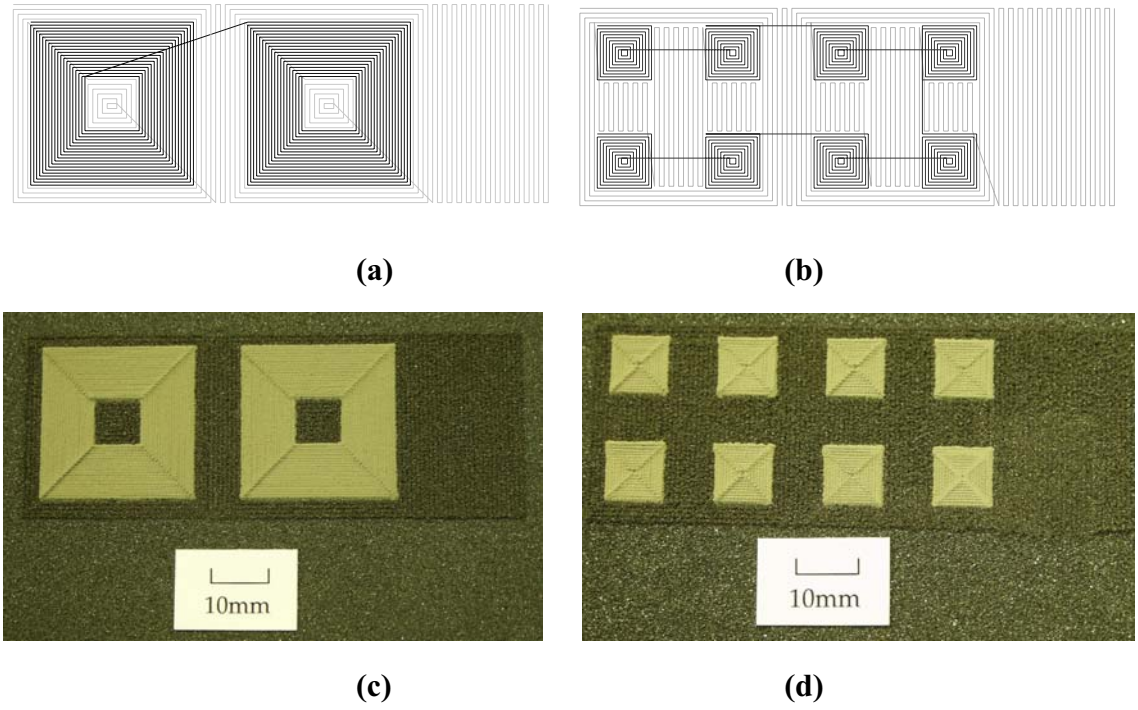

Figure 5 (a) (b)Vector scanning strategies for area fill and (c) (d) co-filled graphite and steel powder blanket on SiC grinding paper. In (a) and (b), the dark lines represent the track of steel and the light lines represent the track of mould/core powder. The lines linking two filled area only represent the motion route; the powder valve is closed.

In order to find the ideal part-mould powder track distance, a step wedge test piece was designed. The track distance was varied at each step from 0.8mm to 1.1mm. The step test piece was infiltrated with bronze and sliced vertically to examine the steps as shown in Figure 7. From right to left the track distance of the step is 0.8, 0.9, 1.0 and 1.1mm. Notice that the 'hill' effect is present on the 0.8mm step and the 'valley' effect on the 1.1mm. The 0.9mm step offers the best track distance. A similar situation develops at the perimeter of each layer adjacent to the crucible where an improper distance causes hill or valley effects around the wall of the crucible. However, because of imperfect fit between crucible and moving base or piston, there is always slight leakage of powder at the crucible/piston gap and this means that the design must be such that part powder does not extend to the crucible wall.

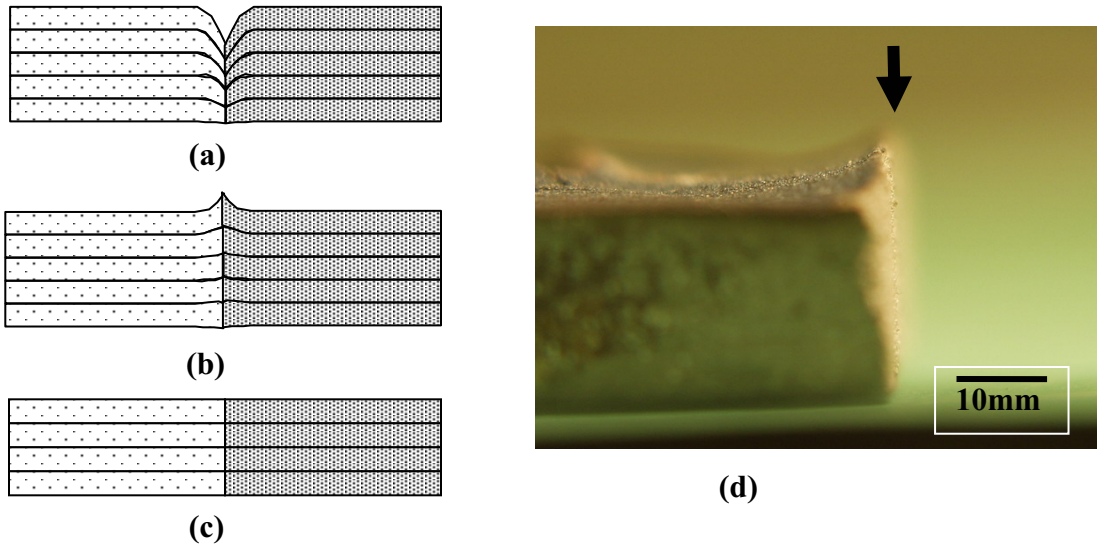

Figure 6 Illustration of defects in the cross section of powder bed. (a) Valley caused by large mould-part powder track distance. (b) Hill caused by small mould-part powder track distance. (c) Ideal powder bed made from optimum mould-part powder track distance. (d) An example of the hill defect (indicated by arrow).

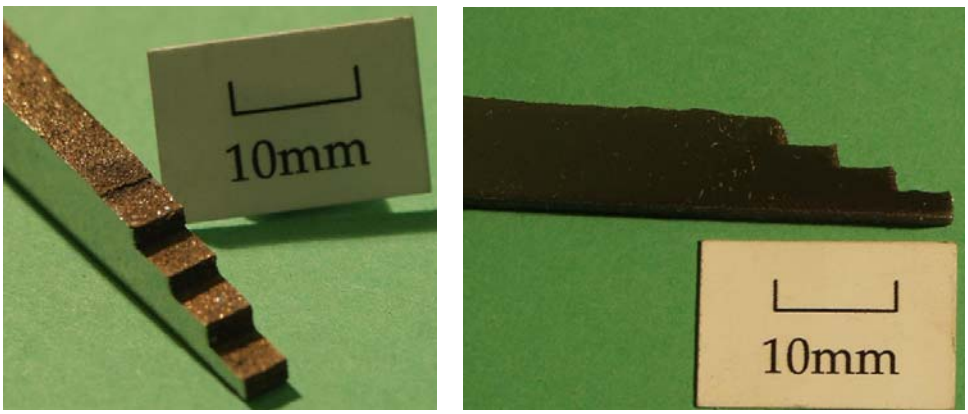

Figure 7 Step wedges fabricated by steel-alumina co-deposition. Fired at 1250°C and infiltrated by bronze. From right to left the track distance of the step is 0.8, 0.9, 1.0 and 1.1mm. Hill effect was present on 0.8mm step and valley effect on the 1.1mm. The 0.9mm is the best track distance.

A test piece of a part/mould/core powder co-deposition is shown in Figure 8. The test piece is a slab of 27× 27×9mm^3 with a vertical square middle hole of 9×9×9mm^3. Both the part/mould (Figure 8 (a))and part/core interface (Figure 8 (b))has flat surfaces. The presence of the core materials did not introduce hot cracks. Ripples presented in the part/mould and part/core interfaces indicated the layered manufacturing. The smooth wall of the graphite crucible gave a smooth but carburized part/crucible surface. A non-ideal part/crucible wall track distance also gives a hill

defect at the edge shown in Figure 8 (a). To avoid the carburization near the wall of the crucible, mould powder was used to insulate the part/crucible thereafter.

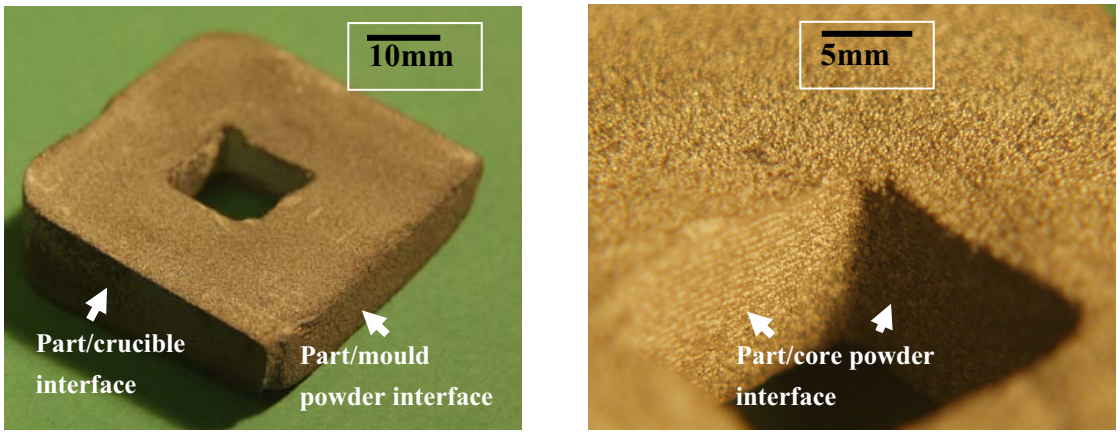

(a) **(b)**

Figure 8 Test piece for a part/mould/core powder co-deposition showing (a) the vertical wall achieved on the part/mould powder interface and (b) the vertical wall of the part/core powder interface.

A test piece of the first order of Menger's sponge was fabricated (**Figure 9**). The Menger's sponge was selected as a test piece to show the capability of complex core fabrication. The horizontal holes were slightly distorted due to mould powder-filling defects (mould powder has higher overrun than the part powder due to the high flowability of the alumina). The defect could be eliminated in further investigations of the filling track parameters of the mould powder.

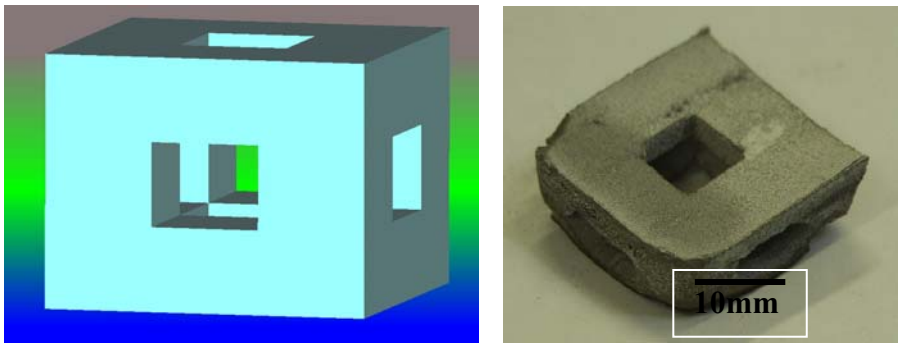

(a) **(b)**

Figure 9. (a) 3D model of Menger's sponge and (b)the test piece fabricated.

Conclusions

A new solid freeforming method based on co-delivery of mould powder materials and part powder materials was demonstrated in this paper. Both coarse alumina powder and graphite powder were tested as the mould/core material. The interface between the dissimilar powders were

investigated. The problem presented by the alumina powder is the entrapment at the surface while the disadvantage of graphite powder is the carburization and powder compaction. The flow rate and switching of the valves provides the composition and shape control during fabrication. Optimization of track width and track distance as well as filling strategy eliminated the fabrication defects. Test pieces including step wedge and Menger's sponge were fabricated with acceptable smooth interfaces. Further investigations are needed on the optimization of remaining fabrication parameters.

Acknowledgments

The authors are grateful to the Engineering and Physical Sciences Research Council for supporting this work under Grant No GR/S74164.

References

1 D.T. Pham and R.S. Gault , A comparison of rapid prototyping technologies, International Journal of Machine Tools and Manufacture, Vol. 38, 1998, 1257-1287.

2 B.Y. Tay, J.R.G.Evans, and M.J. Edirisinghe, Solid Freeform Fabrication of Ceramics, International Matererials Review, Vol.48, 2003, 341-370.

3 A. Vasinonta and J. Beuth, Process Maps for Controlling Residual Stress and Melt Pool Size in Laser-Based SFF Processes. Solid Freeform Fabrication Proceedings, 2000, pp 200-208.

4 M. Matsumoto, M. Shiomi, K. Osakada, F. Abe, Finite element analysis of single layer forming on metallic powder bed in rapid prototyping by selective laser processing, International Journal of Machine Tools & Manufacture, 42, 2002, 61–67.

5 N. Tamari, T. Tanaka, K. Tanaka, I. Kondoh, M. Kawahara, M. Tokita, Effect Of Spark Plasma Sintering on Densification and Mechanical-Properties of Silicon-Carbide, Journal of The Ceramic Society of Japan, 103 (7), 1995, 740-742.

6 J.S. Hirschho, M. Samat, G.M. Maxwell , Induction Sintering Has Potential For Powder Metal Parts, Metal Progress, 97 (5), 1970, 135-&.

7 K.Lappo, B.Jackson, K.Wood, D.Bourell, J.J.Beaman, Discrete multiple selective laser sintering: Experimental study of part processing, Solid Freeform Fabrication Proc. Univ. of Texas, Austin, TX, 2003, pp. 109-119.

8 C.L. Liew, K.F. Leong, C.K. Chua, Z. Du, Dual materials rapid prototyping techniques for the development of biomedical devices, Part 1: Space creation. Int. J.Adv. Manuf. Technol. 18, 2001, 717-723.

9 A.M. Fermier, J. Troisi, E.C. Heritage, M.A. Drexel, P. Gallea, K.A. Swinney, Powder dispensing robot for sample preparation, Analyst, 128, 2003,790-795.

10 J-P.J. Cherng, J. Gonzales-Zugasti, N.R. Kane, M.J. Cima, A.V. Lemmo, Integration of an opto-mechanical mass sensor with a powder-dispensing device for microgram sensitivity, J.Assoc. Lab. Automation, Aug, 2004, 228-237.

11 M. Saito, O. Kimura, N. Yoda, A quantitative powder supply method using ultrasonic vibration, Journal of the Japanese acoustical society. 45, 1989, 38-43.

12 S. Matsusaka, M. Urakawa, H. Masuda, Micro-feeding of fine powders using a capillary tube with ultrasonic vibration, Adv. Powder Technol. 6, 1995, 283-293.

13 Y. Yang, X. Li, Experimental and analytical study of ultrasonic micro powder feeding, J.Phys. D Appl. Phys. 36, 2003, 1349-1354.
14 S. Yang, J.R.G. Evans, Computer control of powder flow for solid freeforming by acoustic modulation, Powder Technol. 133, 2003, 251-254.
15 V.V. Yahchuk, A.O. Sushkov, D. Budker, E.R. Lee, I.T. Lee, M.L. Perl, Production of dry powder clots using a piezoelectric drop generator, Rev. Sci. Instrum. 73, 2002, 2331-2335.
16 P. Kumar, E. Beck, S. Das, Preliminary investigations on the deposition of fine powders through miniature hopper-nozzles applied to multi-material solid freeform fabrication, Solid Freeform Fabrication Proceedings, Austin, Texas 2003, pp. 82-92.
17 A.V. Kumar, H. Zhang, Electrophotographic powder deposition for freeform fabrication, Solid Freeform Fabrication Proceedings, Austin, Texas 1999, pp.647-653.
18 C.L. Liew, K.F. Leong, C.K. Chua, Z. Du, Dual material rapid prototyping techniques for the development of biomedical devices. Part 2: Secondary powder deposition, International Journal Of Advanced Manufacturing Technology, 19 (9): 2002, 679-687.
19 C. van der Eijk. T. Mugaas, R. Karlsen, O. Asebo, O. Kolnes and R. Skjevdal, Metal printing process development of a new repid manufacturing process for metal parts. Proceedings of the world PM2004 conference, Oct 17-21, 2004, Vienna
20 S.J. Rock and C.R. Gilman. A New SFF Process for Functional Part Rapid Prototyping and Manufacturing: Freeform Powder Molding. 1995 Solid Freeform Fabrication Symposium, August 7-9, The University of Texas at Austin, Austin, Texas.
21 S.J.Rock, C.R.Gilman, Method of producing solid parts using two distinct classes of materials, US Pat. 5555481, Sept. 10th 1996, Assign: Rensselaer Polytechnic, Troy, NY.
22 J. Pegna, Exploratory investigation of solid freeform construction, Automation in Construction, 5, 1997, 427-437.
23 J. Pegna, S. Pattofatto, R. Berge, C. Bangalan, H. Herring, M. LeSaux, J. Engler. “The sand painter: two dimensional powder deposition”. Solid Freeform Fabrication Proceedings, Austin, Texas 1997. pp 695-710.
24 S. Yang, M.M. Mohebi, J.R.G. Evans, A novel solid freeforming method based on mould and part co-deposition, to be published.
25 S. Yang and J.R.G. Evans, A multi-component metering and dispensing system for 3D functional gradients, Materials Science and Engineering A 379, 2004, 351-359
26 S. Yang, J.R.G. Evans, Acoustic control of powder dispensing in open tubes. Powder Technology 139 (2004, 55–60
27 J.H. Song and J.R.G. Evans, The Assessment of Dispersion of Fine Ceramic Powders for Injection Moulding and Related Processes, J. Euro. Ceram. Soc. 12, 1993, 467-478.
28 S. Yang and J.R.G. Evans. On the rate of descent of powder in a vibrating tube. Philosophical Magazine, 85 (10), 2005, 1089-1109.
29 S. Yang and J.R.G. Evans. Automated sand painting. To be published.
30 J.L. Johnson, Principles of computer automated fabrication. Palatino Press, 1994, p11.